

Resistance to Water Flow in Xylem Vessels

AYODEJI A. JEJE¹ AND MARTIN H. ZIMMERMANN

Harvard University, Harvard Forest, Petersham, Massachusetts 01366

Received 1 November 1978

ABSTRACT

Experimental data on flow resistances in xylem vessels with different lumen wall surface sculptures are presented. The technique involved using determinable forces at menisci to pull water through isolated undamaged metaxylem and protoxylem vessels which were empty but had water-saturated walls. In the horizontal orientation, the surface tension forces moved the water at velocities that the resisting viscous forces at the vessel walls would allow since inertial forces were found negligible. A high speed camera was used to determine the meniscus translation rates. Vessel diameters as well as average dimensions of the microscopic internal surface irregularities were measured with respect to axial position from the inlet. From these, flow resistances were determined in terms of dimensionless friction factor, f , as functions of Reynolds number, Re .

It was found that, at certain helical ring thicknesses and spacing, resistance to flow was lowest. Deviations from these parameter values cause dramatic increases in resistance to flow. Results are applicable to normal flow in plants, i.e. without menisci present.

INTRODUCTION

Xylem vessels are closed-ended microcapillaries of various lengths organized into intricate network structures for water conduction over relatively long distances in most higher land plants. Each vessel, a string of vessel elements with a continuous lumen divided at intervals by perforation plates of varying geometry and porosity, is a solid but porous shell of oriented cellulosic strands interspersed with numerous apertures, or pits, through which spatial connections are made to adjoining vessels for flow continuity (Esau, 1965; Frey-Wyssling, 1976). The pits are usually concentrated in the region of overlap between juxtaposing but axially displaced vessels. The channel of least bulk flow resistance is from vessel lumen-to-lumen through pit pairs.

Major resistances to water movement from the roots to the apical sections of a plant are provided by gravity, friction drag at the vessel walls, and form drag both at the perforation plates (between vessel elements) and pit areas (between vessels). The friction and form drags are in alternating series with the overall magnitude dependent on the flow rates along a particular path, the frequency of both pit areas and perforation plates (inversely proportional to the longitudinal dimensions of the vessels and vessel elements respectively), the population and dimensions of the pits, as well as the geometry of the perforation plates.

¹ On leave from University of Lagos, Nigeria

The internal surface lumen walls are usually microscopically irregular with pits and varying amounts of cellulose deposited on primary walls as rings, spirals, or reticulate secondary wall thickening representing sculptures over which sap must flow. Van der Graaf and Baas (1974) and Carlquist (1975) have reported an increase in the incidence of helical vessel thickening with latitude and altitude. The former also reported an observation of the miniaturization of the secondary xylem elements (shorter vessel members and narrower vessels) as one progresses from the tropics to colder temperature zones, and the restriction of helical thickening to narrow mature vessels (e.g. 10–50 μm in *Ailanthus glandulosa*) in the tropics. They noted that often helical thickenings are better developed in or are entirely limited to the constricted ends of vessels as compared to parts of larger diameters.

In translocation literature, various floating correction factors have been and are being used to compare translocation in the xylem vessels to fully developed laminar flow in ideal capillaries with non-porous walls (Berger, 1931; Münch, 1943; Riedl, 1937; Zimmermann and Brown, 1971; Zimmermann, 1978; Giordano, Salleo, Salleo, and Wanderlingh, 1978). In many plants, a wide range is found for the factors, even for segments on the same branch. Sometimes based on the factor values, the xylem conducts as well or even better than uniform bore, straight and smooth-walled capillaries even though, in the xylem, the pit areas present significant hindrance to bulk flow.

This study is an attempt to relate the above observations and to present a fundamental approach for studying flow resistances in plant vascular tissue. Certain wall configurations are proposed to be functionally adapted to reduce friction drag to different degrees. In general, for flows in tubes, normal surface irregularities of small dimensions relative to the diameter of the conduit do not have noticeable effects on laminar motion (Bird, Stewart, and Lightfoot, 1960). However, for pronounced protrusions into the lumen, as for the orifice plates used industrially to measure pipe flow rates, flow patterns and resistances are significantly affected. For a series of separated but closely spaced orifice plates of similar apertures within a pipe, the effective flow diameter is that defined by the aperture openings. Flow resistance is intermediate between that for a solid tube of identical wetted surface area and length, and a confined free jet with regulated vorticity generation at the boundary. In a related problem but with a different configuration, Taylor (1971) experimentally demonstrated that the force required to sustain a fluid motion decreases when the boundary contains grooves within a given range of dimensions. In the xylem, some configurations of secondary thickening provide grooves in between and consequently a reduction in the tangential surface stresses resisting flow at the effective capillary boundary is possible. The overall effect would be a limited 'slip' flow and the lowering of friction drag. Experiments are described here on the study of this phenomenon in isolated xylem vessels.

MATERIALS AND METHODS

The apparatus comprises four major components: isolated strands of xylem vessels of *Plantago major* L., a microscope, a high speed camera and a high intensity illumination (Fig. 1A). Fibro-

vascular bundles which consist of rows of xylem vessels are readily dissected out of the petiole of the *Plantago* leaf (Plate 1). The isolation of the xylem strands without appreciably changing the configuration from that existing in the live plant proceeded after the surrounding fibre cells had been softened in one of two ways. Segments (2–3 cm long) of the cylindrical bundles were then made into circular loops, held with forceps near the open ends, and then partially immersed (excluding the cut ends) in concentrated sulphuric acid for a maximum of 5 s until they became just limp. They were then immediately transferred into three consecutive distilled water baths where they turned opaque white. They were allowed to soak for a minimum of 12 h before further treatment. The alternative was to leave the untreated cut segments in a covered Petri dish for about 2 d when, presumably, bacterial action resulted in the fibre softening. Either way, no differences are noted in the usefulness of or results from the samples. When a softened segment is put between two glass slides with some drops of water and pressed flat, the fibres are displaced sideways to reveal the xylem vessels. These

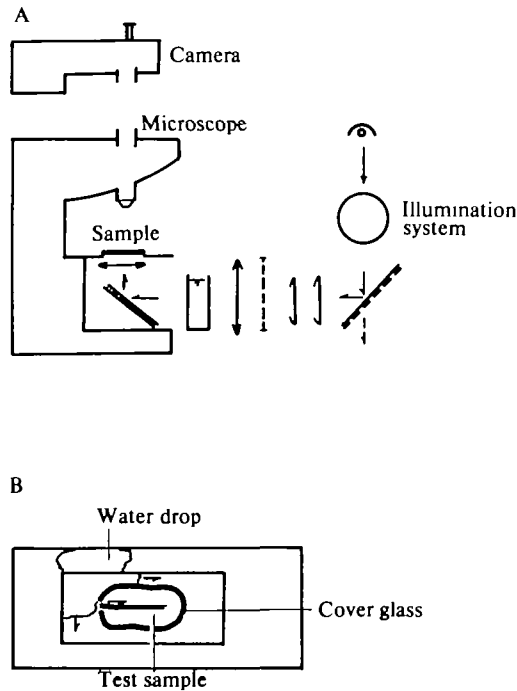
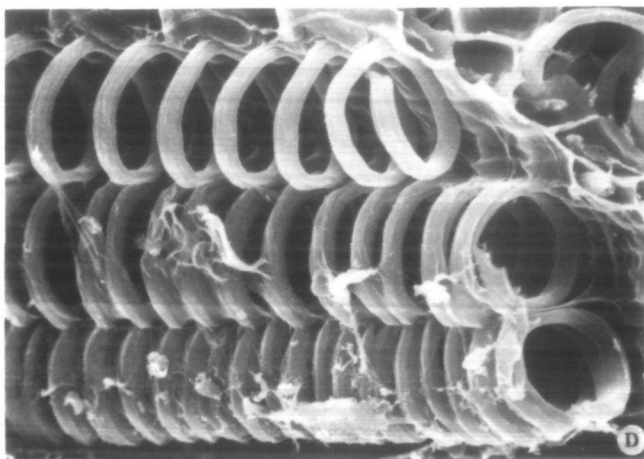
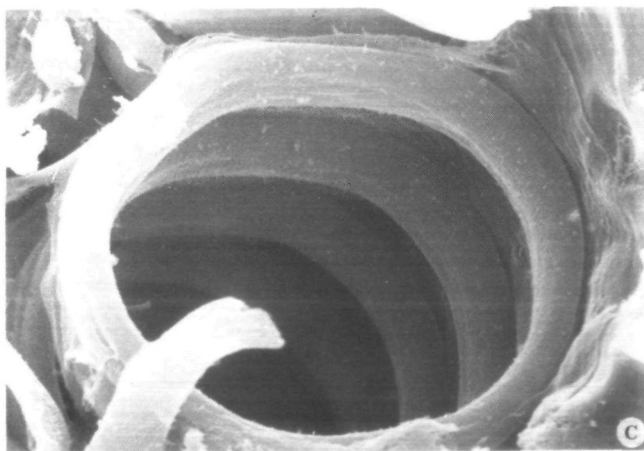
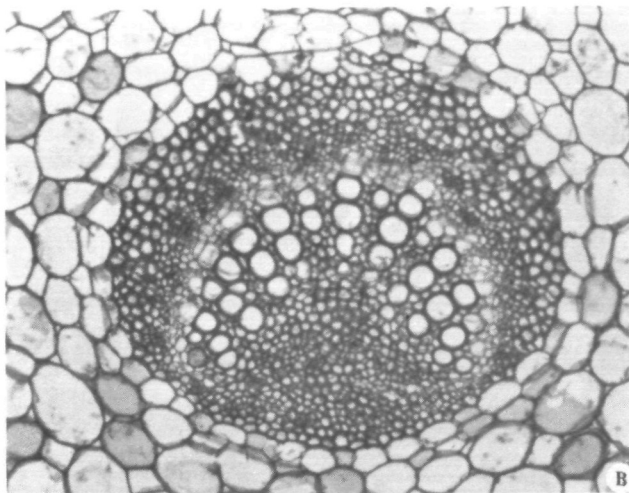
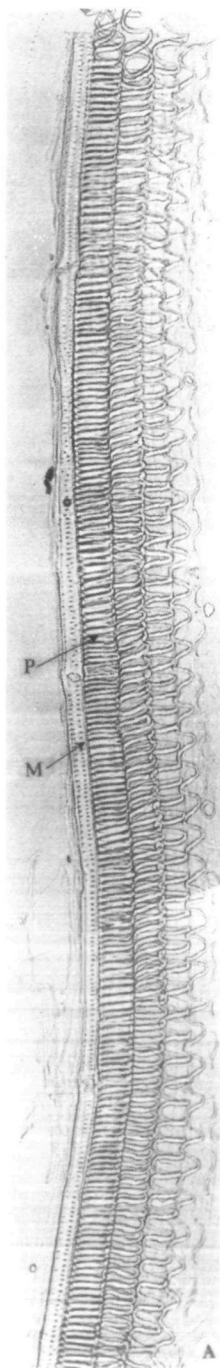


FIG. 1A. Diagram of set-up. B. Experimental sample.

were separated under a stereomicroscope with glass capillaries flame-drawn to fine points. Vessel lengths of 5–8 mm were dissected out. Samples with either the primary walls absent or damaged were discarded. Good samples with 1–5 contiguous vessels of different dimensions were placed on clean glass slides, still wet, and ringed with less useful or damaged xylem strands as in Fig. 1B for reasons to be discussed later. Cover plates were tacked down in position with small droplets of a special fingernail polish at two opposite corners of the plates. To keep the samples from drying out (and primary walls from cracking) until ready for use, they were kept in a covered desiccator jar with a pool of water at the bottom.

Light from a 300 W tungsten-halogen lamp equipped with a dichroic reflector was passed through a 10 cm thick dilute copper sulphate solution heat filter before its path was changed 90° with a cold mirror. The mirror transmitted about 80% of the incident heat and reflected 90% of the visible radiation. The emergent beam was collimated with a series of lenses, passed through an i.r. glass filter, and a 1 cm thick layer of cold water, before being reflected to the stage of a Wild M20 microscope. The light passed through a long-working-distance condenser (N.A. 0.52), the sample on the stage, and a $\times 6$ Plan Fluotar objective before reaching the high speed camera, a Redlake HYCAM model equipped with 1000/100 Hz timing light generators, aligned above. No projective



lens was used on the microscope and no lens on the camera. Effective field of sample view was approximately 1 mm × 0.75 mm on the full 16 mm film frame.

At the start of a run, the prepared sample was positioned with the inlet end of the vessel and as long a section as possible visible in the camera. Water under the slide cover was allowed to evaporate. Eventually most of the water disappeared. The experiment proceeded immediately when the vessels had become empty but while the walls were still moist and patches of water were under the cover plate. A drop of water from a syringe was placed at one edge of the cover plate parallel to the xylem vessel(s) orientation. The camera was activated simultaneously at frame rates of 200 or 500 s⁻¹. Capillary action moved the water toward the sample rapidly under the cover plate. The ring loop drawn around the test sample prevented water touching the entire vessel simultaneously. At time zero, water contacted the vessel inlet and an internal meniscus formed. Liquid front motion towards the sample under the cover plate was essentially at right angles to that which would occur in the xylem vessels, therefore the approach velocity was in a direction normal to the inlet, and hence fluid inertial force was made negligible. Flow in the xylem vessels was then controlled by surface tension forces of known value at the moving meniscus from the instant when water touched the vessels (Plate 2C, D). Resistance was determined from an overall momentum balance on the system. This involves formulating an equation for the force field acting within the system in terms of the surface tension, viscosity, inertia, gravity, and pressure. The resulting expression is solved after appropriate simplifications and boundary conditions are introduced. Contact angles were assumed to be zero in view of the high affinity of cellulose for water. Inertial forces proved to be negligible.

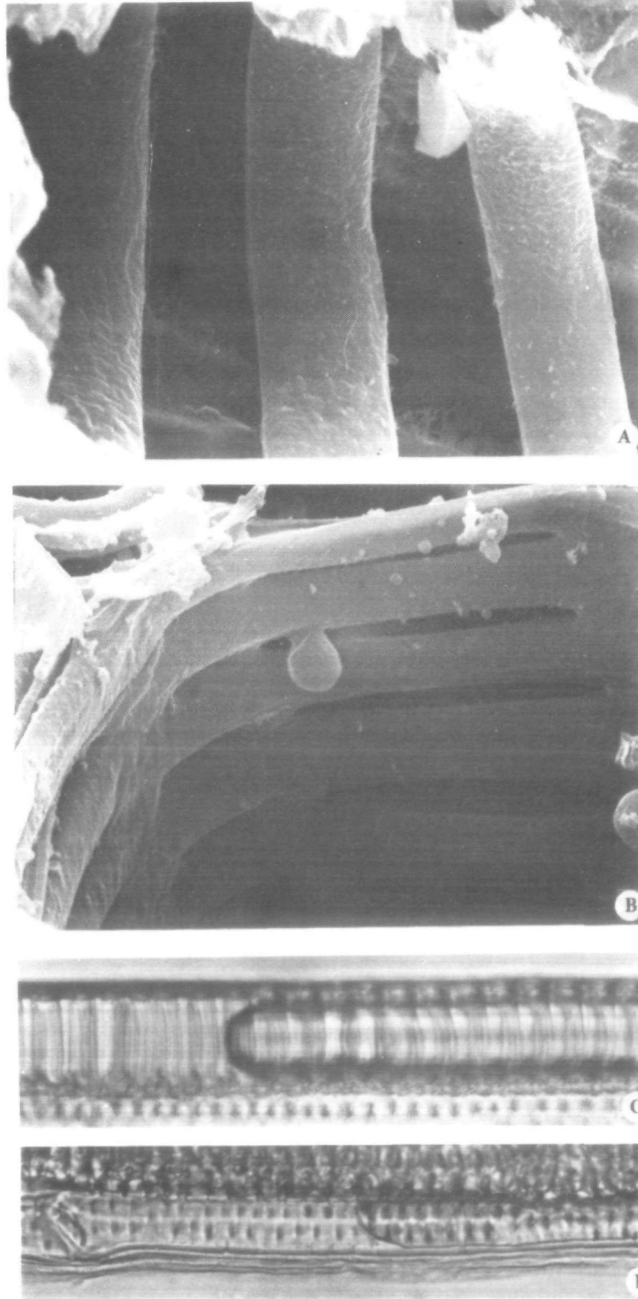
The films were analysed frame by frame on a 16 mm L & W Analyser. The results and discussion are presented in the following sections.

RESULTS

Typical distance (from inlet to meniscus position) versus time data are presented in Fig. 2 for protoxylem (P) and metaxylem (M) with perforation plates. These vessels are the same as marked in Plate 1A. The meniscus moved relatively smoothly in the protoxylem with predictable lowering of translation velocity as the capillary wetted area increases, although the diameter (measured as shown in Fig. 3) oscillated between 18.5 and 22.6 μm for the test section. The metaxylem plot exhibits an acceleration at about 250 μm from inlet—in the divergent region soon after the visible constriction to about half the diameter up- and downstream. The meniscus was temporarily halted at about 475 μm, and at 770 μm where perforation plates were located. The first perforation plate at 173 μm did not retard the meniscus motion, presumably because its orientation is almost normal to the flow axis, and the fact that the perforation plate aperture is of the same order of magnitude as the vessel diameter upstream. (Vessel element ends appear generally wider than at other locations for the specimens of this study.) Again vessel diameters at different distances from inlet varied from 5.4 μm to 11.6 μm with occasional sharp convergent and divergent sections.

The raw data were fitted with polynomial regression equations in overlapping blocks. The first derivatives of resulting expressions yield local translation velocities, U , of the meniscus and the liquid in its wake. Using the local radius, r , at

PLATE 1. Xylem vessels of *Plantago major* L. A. Isolated strands of vessels showing from right to left development progression from vessels with widely separated secondary rings to closely spaced helical rings in protoxylems, and a metaxylem with perforation plates (×248). B. Cross-section of a *Plantago* vascular bundle excised from leaf petiole. The vessels outermost of the crescent arrangement are metaxylem (×260). C. Scanning electron micrograph of a protoxylem vessel. Both the helical thickening and the primary walls are shown. The ring thickness is a significant fraction of the vessel diameter (×5200). D. Another scanning electron micrograph showing helical thickening and spacing more clearly. Remnants of the primary walls, torn in the preparation, are visible on the lower two vessels (×1400).



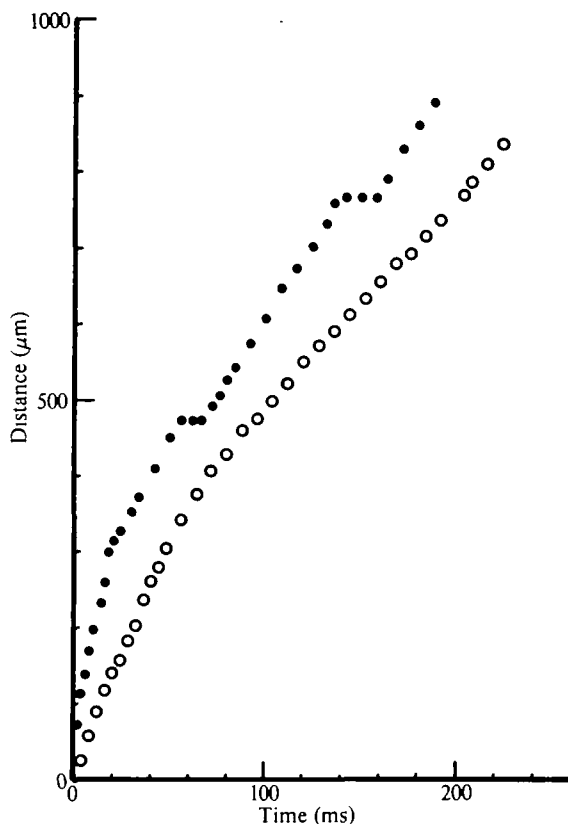


FIG. 2. Typical meniscus distance (from inlet) versus time data for water (temperature 25 °C) movement in metaxylem (●) and protoxylem (○) vessels. The test specimens for the data presented are shown in Plate 1A.

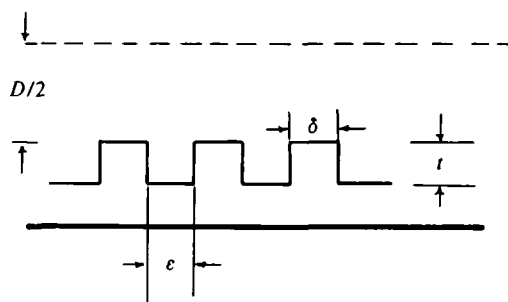


FIG. 3. Idealized form of lumen wall sculpture for xylem vessels. The thickness of the secondary wall in the radial and axial directions, and the separation distance between rings are represented by t , δ , and ϵ respectively. The capillary diameter from the surface of the secondary wall is denoted by D .

PLATE 2. A. Scanning electron micrograph of a *Plantago* protoxylem segment. The primary walls had been subjected to stresses during sample preparation as evidenced by some local tears. Secondary rings appear to have rounded cross-sections. Ring spacing is shown to be irregular ($\times 6600$). B. A scanning electron micrograph of a metaxylem not fully formed. Secondary rings have been bridged in many locations ($\times 5800$). C, D. Menisci pulling water through *Plantago* vessels. In protoxylems, the meniscus outline is usually hemispherical. The moving liquid/solid/gas contact line appears to be retarded at pits in many metaxylem vessels and the meniscus assumes irregular shapes. For the experiments, only data for those with hemispherical outlines are reported ($\times 980$).

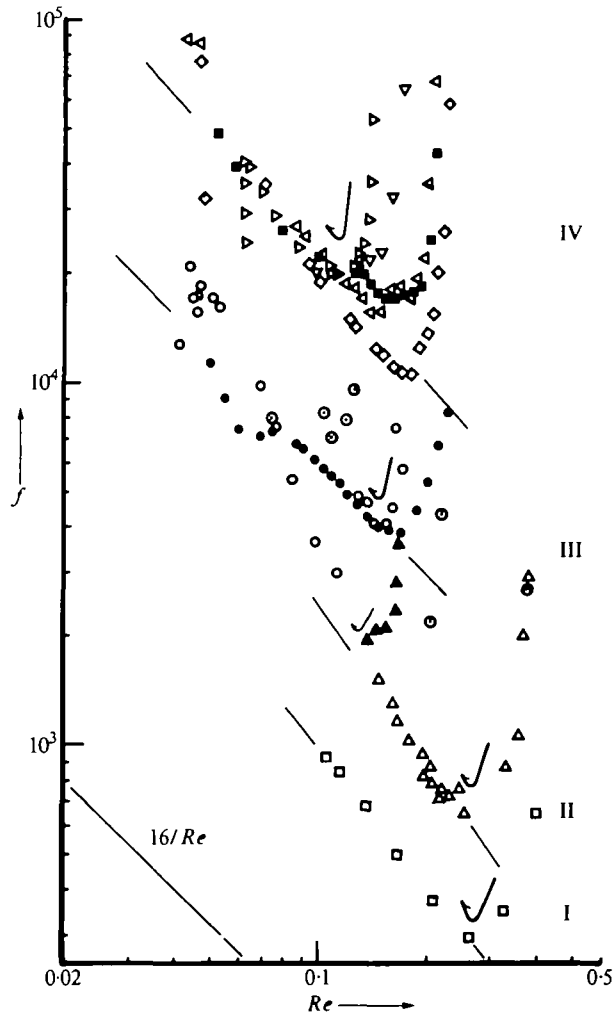


FIG. 4. Plots of friction factor f versus Reynolds number Re for water flow in xylem vessels at 25 °C.

Parameters	$\delta/(\delta + e)$	t/D	δ	Vessels
Groups				
I	0.45	0.19	2.3 μm	Protoxylem
II	0.25	0.184	2.3 μm	Protoxylem
III	—	—	—	Metaxylem
IV	>0.6	<0.1	>8 μm	Protoxylem

Flow in an ideal nonporous noncellulosic capillary is represented by the straight line $f = 16/Re$.

the position of the meniscus and average diameter, D , for the tube over the wetted length, L , a dimensionless friction factor for flow in a straight, relatively uniform conduit, f_s , is computed from

$$f = \frac{4\sigma r}{\rho U^2 DL}$$

where σ and ρ are gas/liquid interfacial tension and liquid density respectively. This is a ratio of the flow driving pressure and the dynamic pressure. This parameter is plotted versus the dimensionless Reynolds number, Re , ($DU\rho/\mu$, where μ is the liquid viscosity coefficient) in Fig. 4. On the same plot is drawn the curve for horizontal glass capillaries with a meniscus pulling the liquid through. It has been experimentally demonstrated that this line is essentially the same as obtained for steady laminar flow through ideal capillaries for the vessel diameters under consideration (Jeje, 1979). The discussion of these results follows after definition of some terms.

DISCUSSION

The sculpture of the lumen internal walls is represented with a crude approximation in Fig. 3 to define measurement parameters, especially for protoxylem vessels. The projected width of secondary wall deposits are denoted by δ while ϵ is the spacing between the ring or loops. It should perhaps be stressed that the cross-section of the secondary walls are by no means rectangular, varying between upright and inverted triangles without sharp corners. Usually they assume a rounded outline as shown in Plate 2A and B.

Over a given vessel length, both δ and ϵ vary arbitrarily although within certain limits for any particular vessel, hence average values can be determined for the short segments examined. The thickness of the secondary rings is denoted by t and the vessel diameter D at any location is measured over the secondary deposits. One parameter that was not examined here is the angle of orientation of secondary rings and spirals to the flow axis. The angles are observed to change arbitrarily over short segments. Abrupt changes are observed to effect the rates of meniscus translation, although the present understanding indicates second-order effects on flow resistance. The transition between protoxylem and metaxylem (Plate 2B) shows bridges between rings. The parameters for these were based on local averaged values.

The metaxylem vessels have periodic oval slits in between the 'original' secondary layer deposits. These slits occasionally cause retardation of the movement of the meniscus wall contact line as suggested by uneven meniscus curvature in Plate 2D. The protoxylem meniscus was almost always hemispherical, suggesting a zero dynamic contact angle.

The results in Fig. 4 fall within four groups based on the parameter values. The general pattern is that friction factor values are initially high and fall rapidly with regard to the Reynolds number. The factor achieves a minimum and then rises again as the Reynolds number decreases. Similar results were obtained for glass capillary tubes (Jeje, 1979). In the latter study, it was demonstrated that a vortex motion (with an attendant increase in flow resistance) was generated in the wake of the meniscus. Such vortices are not normally present in flow in ideal capillary tubes without a free surface in motion. Hence it was of importance to demonstrate that the present technique does yield answers to the posed problem and not other undefined ones. Data and visual demonstrations with glass capillary tubes show that, after the meniscus had pulled far from vessel inlet, the vortex (or secondary

motion) dissipates. Except for small segments in the immediate wake of the meniscus and at the vessel inlet zone, the major portion of liquid column essentially approximated fully developed laminar flow at the appropriate Reynolds number. The friction factor is defined by the line $f = 16/Re$. Hence the portion of the data in Fig. 4 with negative slope is that corresponding to fully developed laminar flow approximations for xylem vessels. As shown, the data essentially fall on straight lines for the useful portions.

With this background, one can examine the curves in Fig. 4. The groupings are for different vessel diameters and sculpture characteristics. Parameters found useful are $\delta/(\delta + \epsilon)$, t/D , and average δ (or ϵ) values. The first is the ratio of the secondary wall thickness for adjacent rings; t/D denotes ratio of wall protrusions to vessel lumen diameter. The absolute values of δ (or ϵ) are also required to fully define the idealized internal surface forms.

The curve in group I exhibits the high starting f values which decreased and then increased as the flow Reynolds number dropped (in the direction of the arrow) in an experiment. As noted earlier, the useful portion for the present purposes is the straight line portion with negative slope. It represents the resistance to fluid motion contributed primarily by the vessel walls. As compared to data for steady laminar flow in uniform straight non-porous capillary tubes, the resistance to motion is higher for the protoxylem vessel. This curve reproduced in repeated runs, however, shows the lowest resistance to motion for all the samples tested. The averaged parameter values are $\delta/(\delta + \epsilon) = 0.45$, $t/D = 0.19$, and $\delta = 2.3 \mu\text{m}$. The spacings between rings and secondary wall thickness are small and are of the same order of magnitude. Secondary wall protrusion above the primary wall is noticeably significant.

When t/D and δ assume the same order of magnitude in group II but the $\delta/(\delta + \epsilon)$ is lower, a higher resistance to flow is recorded. This is attributed solely to an increase in wall surface area over which the stresses resisting the motion act per unit length of vessel. Presumably a limited 'slip' flow occurs over the water-filled gaps between adjacent rings.

For metaxylem vessels when the ring spacings have been bridged and mostly covered over with cellulosic deposit to yield relatively smooth lumen walls (group III) the resistance to fluid motion is higher still. Data from different experiments clustered about a mean line. Resistance to motion posed by perforation plates are second-order effects in this study when the flow is maintained, that is, when temporary halts in meniscus translation at the perforation plates are neglected. The configuration for the metaxylem is closest to that of a non-porous uniform capillary tube, although the secondary rings are not completely merged and pits are periodically spaced (Plate 2D).

Group IV contains the largest cluster of data presented and it embodies a large variation in surface structure. Samples with ring spacing ϵ around 8–10 μm and wider for $t/D < 0.2$ showed results in this range irrespective of the $\delta/(\delta + \epsilon)$ values. Data for large $\delta/(\delta + \epsilon) \sim 0.8$ and small $t/D < 0.1$ also fell in this region even for small $\epsilon \sim 1 \mu\text{m}$. These suggest that more wetted area than estimated by using D (as in Fig. 3) is utilized in resisting fluid motion. The possibility of energy losses due to

small vortices formed in the neighbourhood of the secondary deposits must also be considered.

Thus the general pattern is that, as the ring thickness to vessel diameter, t/D and $\delta/(\delta + \varepsilon)$ decrease and ring spacing ε increases, the resistance to liquid motion in the xylem increases. Certain combinations of the above parameters as in group I yield the lowest resistance to water movement in xylem capillaries. Also the porosity of the xylem walls affects the flow rates either by lateral water injection into (or withdrawn from) the main bulk flow, or by an as yet unexplained interaction between the meniscus actuating the motion and the vessel walls.

As is apparent, the straight line portions of the results in Fig. 4 are directly applicable for normal flow in plants where menisci (free surfaces) are absent; as long as geometric similarity for the wall sculpture is obtained for the vessel of interest and those in the figure at appropriate Reynolds numbers.

ACKNOWLEDGEMENTS

This work was carried out while the first author held a Bullard Fellowship at Harvard University. We gratefully acknowledge the assistance of Barbara Zimmermann and Monica Mattmüller at various phases of this study.

LITERATURE CITED

- BERGER, W., 1931. *Beih. bot. Zbl.* **48**, 363–90.
- BIRD, R. B., STEWART, W. E., and LIGHTFOOT, E. N., 1960. *Transport phenomena*. J. Wiley & Sons, N.Y.
- CARLQUIST, S., 1975. *Ecological strategies of xylem evolution*. Univ. Calif. Press, Berkeley, L. A., London. P. 102.
- ESAU, K., 1965. *Plant anatomy*. 2nd Edn. J. Wiley & Sons, N.Y.
- FREY-WYSSLING, A., 1976. *The plant cell wall*. 3rd Edn. Encyclopaedia of Plant Anatomy, Band III, Teil 4, Gebrüder Borntraeger, Berlin.
- GIORDANO, R., SALLEO, A., SALLEO, S., and WANDERLINGH, F., 1978. *Can. J. Bot.* **56**, 333–8.
- JEJE, A., 1979. *J. Colloid Interface Sci.* (in press).
- MÜNCH, E., 1943. *Flora*, **136**, 223–62.
- RIEDL, H., 1937. *Jb. wiss. Bot.* **85**, 1–72.
- TAYLOR, G. I., 1971. *J. Fluid Mech.* **49**, 319–26.
- VAN DER GRAAFF, and BAAS, P., 1974. *Blumea*, **22**, 101–21.
- ZIMMERMANN, M. H., 1978. In *Tropical trees as living systems*. Eds. P. B. Tomlinson, and M. H. Zimmermann. Pp. 517–32.
- and BROWN, C. L., 1971. *Trees: structure and function*. Springer-Verlag, N.Y. Pp. 196–9.